The American Journal of Pathology, Vol. 182, No. 3, March 2013

The American Journal of
PATHOLOGY
ajp.amjpathol.org

MUSCULOSKELETAL PATHOLOGY

Loss of β-Catenin Induces Multifocal Periosteal Chondroma-Like Masses in Mice

Leslie Cantley,* Cheri Saunders,* Marta Guttenberg,† Maria Elena Candela,* Yoichi Ohta,* Rika Yasuhara,‡ Naoki Kondo,‡ Federica Sgariglia,* Shuji Asai,* Xianrong Zhang,§ Ling Qin,§ Jacqueline T. Hecht,¶ Di Chen,‖ Masato Yamamoto,** Satoru Toyosawa,†† John P. Dormans,§‡‡ Jeffrey D. Esko,§§ Yu Yamaguchi,¶¶ Masahiro Iwamoto,*§ Maurizio Pacifici,*§ and Motomi Enomoto-Iwamoto*§

From the Translational Research Program in Pediatric Orthopaedics, the Department of Pathology and Laboratory Medicine,† and Division of Orthopedic Surgery,‡‡ Department of Surgery, Children's Hospital of Philadelphia, Philadelphia, Pennsylvania; the Department of Orthopaedic Surgery,‡ Thomas Jefferson University, Philadelphia, Pennsylvania; the Department of Orthopedic Surgery,§ School of Medicine, University of Pennsylvania, Pennsylvania; the Division of Medical Genetics,¶ Department of Pediatrics, The University of Texas Medical School at Houston, Houston, Texas; the Department of Biochemistry,‖ Rush University, Chicago, Illinois; the Department of Surgery,** University of Minnesota, Minneapolis, Minnesota; the Department of Oral Pathology,†† Graduate School of Dentistry Osaka University, Suita, Japan; the Department of Cellular and Molecular Medicine,§§ University of California San Diego, La Jolla, California; and the Sanford Children's Health Research Center,¶¶ Sanford-Burnham Medical Research Institute, La Jolla, California

Accepted for publication November 7, 2012.

Address correspondence to Motomi Enomoto-Iwamoto, D.D.S., Ph.D., Translational Research Program in Pediatric Orthopaedics, Division of Orthopedic Surgery, Department of Surgery, Children's Hospital of Philadelphia, 3615 Civic Center Blvd., ARC902, Philadelphia, PA 19104. E-mail: iwamotom1@email.chop.edu.

Osteochondromas and enchondromas are the most common tumors affecting the skeleton. Osteochondromas can occur as multiple lesions, such as those in patients with hereditary multiple exostoses. Unexpectedly, while studying the role of β-catenin in cartilage development, we found that its conditional deletion induces ectopic chondroma-like cartilage formation in mice. Postnatal ablation of β-catenin in cartilage induced lateral outgrowth of the growth plate within 2 weeks after ablation. The chondroma-like masses were present in the flanking periosteum by 5 weeks and persisted for more than 6 months after β-catenin ablation. These long-lasting ectopic masses rarely contained apoptotic cells. In good correlation, transplants of β-catenin-deficient chondrocytes into athymic mice persisted for a longer period of time and resisted replacement by bone compared to control wild-type chondrocytes. In contrast, a β-catenin signaling stimulator increased cell death in control chondrocytes. Immunohistochemical analysis revealed that the amount of detectable β-catenin in cartilage cells of osteochondromas obtained from hereditary multiple exostoses patients was much lower than that in hypertrophic chondrocytes in normal human growth plates. The findings in our study indicate that loss of β-catenin expression in chondrocytes induces periosteal chondroma-like masses and may be linked to, and cause, the persistence of cartilage caps in osteochondromas. *(Am J Pathol 2013, 182: 917–927; http://dx.doi.org/10.1016/j.ajpath.2012.11.012)*

Osteochondromas and enchondromas are the most common tumors affecting the skeleton.[1,2] Osteochondromas are cartilage-covered masses that form near the growth plate and bone surface, whereas enchondromas form within the growth plate and bone marrow. Both types of benign tumors can cause mechanical impairment of movement and also pain due to impingement or compression of nerves and blood vessels, particularly when they are present at multiple sites.[3,4] These benign tumors may become malignant.[5–7] The potential for malignant progression is greater in patients with syndromes, such as Ollier disease, Maffucci syndrome, or hereditary multiple exostoses (HME), the latter also known as multiple osteochondroma.[5–7] Current treatments largely rely on surgical excision.[3,8] Both benign and malignant cartilage tumors are generally resistant to chemotherapy and radiotherapy.[5,9] Thus, a better understanding of the cellular and molecular mechanisms underlying cartilage tumor formation and growth is critical for the development of new therapeutic strategies and treatments.

Supported by NIH grants AR058382 (M.P.), AR061758 (M.P.), AR062908 (M.P.), GM33063 (J.E.), and a Foerderer Award (FY2012) from the Children's Hospital of Philadelphia (M.E.-I.).

A guest editor acted as editor-in-chief for this manuscript. No person at Thomas Jefferson University was involved in the final disposition of this article.

http://dx.doi.org/10.1016/j.ajpath.2012.11.012

Recent studies have indicated that several genes play important roles in cartilage tumor formation.[4,5] Hopyan et al[10] found mutations in parathyroid hormone receptor 1 (*PTHR1*) in patients with multiple enchondromas. These authors generated mice harboring the same *PTHR1* mutations that displayed a similar enchondroma formation. In addition, they found that the *PTHR1* mutations caused constitutive activation of hedgehog signaling in cultured chondrocytes and that overexpression of Gli2, a downstream molecule of hedgehog signaling, induced enchondromas in mice.[10] In the follow-up studies, however, it was found that certain cohorts of enchondromatosis patients do not have *PTHR1* mutations[11] and that enchondroma formation may actually be independent of hedgehog signaling.[12] Thus, the pathogenesis of enchondroma formation remains to be clarified.

Mutations in *EXT1* and *EXT2* genes have been associated with hereditary multiple exostoses (HME) (multiple osteochondroma).[5–7] Mutations in these genes are often missense or frame shift and cause synthesis of lower levels of (and shorter) heparan sulfate chains.[4,5] This is because *EXT1* and *EXT2* encode Golgi-associated enzymes are responsible for the polymerization of the chains.[13] Insufficiency of heparan sulfate-rich proteoglycans is thought to be a cause of osteochondroma formation.[4,5,13] Heparan sulfate proteoglycans are important for the regulation of many signaling pathways that include hedgehog, bone morphogenetic protein, fibroblast growth factor, and Wnt pathways.[13,14] All of these pathways are critical regulators for chondrogenic differentiation and chondrocyte differentiation.[15,16] It is likely that dysregulation of these signaling pathways resulting from heparan sulfate deficiency may trigger abnormal behavior of growth plate chondrocytes or induce ectopic chondrogenic differentiation, leading to ectopic cartilage formation. Recently, several *Ext* mutant mouse lines have been established.[17–19] All of these transgenic mouse lines show multifocal ectopic cartilaginous masses with microscopical and structural similarities to osteochondromas found in HME patients.[17–19] The cellular and molecular mechanisms underlying EXT mutation-associated chondroma formation, however, remains largely unclear.

The Wnt/β-catenin signaling pathway is essential for regulation of normal cartilage development, maintenance of permanent cartilage, and growth plate function.[20–24] Previous reports have shown that inactivation of this signaling pathway impairs cartilage and skeletal development. Conditional ablation of the β-catenin gene in limb skeletogenic cells induces a delay in endochondral bone formation and the formation of abnormal cartilaginous masses during embryonic development.[25–27] In addition, overexpression of a Wnt antagonist strongly inhibits both hypertrophy of chondrocytes and progression of endochondral ossification.[28] Recently, we generated compound transgenic mice in which we induced postnatal conditional ablation of β-catenin in cartilage.[24] We found that the resulting β-catenin deficiency impaired growth plate function and skeletal growth. In addition, the mice developed ectopic cartilaginous masses located near the bone surface but not within the bone marrow. In the present study, we characterized the pathohistology of these ectopic cartilaginous masses and investigated their possible cell origin and fate, and also related the findings to human osteochondromas.

Materials and Methods

Transgenic Mice

All mouse studies were conducted with approval by the Institutional Animal Care and Use Committee. *β-catenin$^{fl/fl}$; Rosa-LacZ* mice that harbors floxed *β-catenin* (homo) and Cre-inducible *LacZ* (homo) were generated by mating *β-catenin* floxed mice (*β-catenin$^{fl/fl}$*) possessing LoxP sites in introns 1 and 6 in the *β-catenin* gene (*6.129-Ctnnb1tmKem/KnwJ* line purchased from the Jackson Laboratory, Bar Harbor, ME) with *R26Rosa-lox-stop-lox-LacZ* (*Rosa-LacZ*) mice (*129S-Gt(ROSA)26Sor^{tm1Sor}/J* from the Jackson Laboratory). *Col2CreERβ-catenin$^{fl/fl}$* mice were generated by mating *β-catenin$^{fl/fl}$* mice with *Col2CreER* mice that harbor Cre recombinase, which is linked to a modified estrogen ligand binding domain under the control of *collagen 2a1* promoter sequences. Two independent *Col2CreER* mouse lines, herein referred to as *Col2CreER*[29] and *Col2CreER* (D.C.)[30] were originally generated by Drs. Susan Mackem (National Cancer Institute, Frederick, MD) and Di Chen (Rush University, Chicago, IL) respectively. The *Col2CreER;β-catenin$^{fl/fl}$* mice were mated with the *β-catenin$^{fl/fl}$;Rosa-LacZ* or *β-catenin$^{fl/fl}$* mice, and the resulting littermates received i.p. injections of tamoxifen (100 μg/10 μL per mouse) at day 5, 6 and 7 or day 5 and 7 after birth. The mice were sacrificed at 1, 2, 5, and 8 weeks, or 6 months after completion of the tamoxifen injections. The total number of mice inspected in *β-catenin$^{fl/fl}$* with or without *Rosa-LacZ$^{+/-}$* and *Col2CreER; β-catenin$^{fl/fl}$* with or without *Rosa-LacZ$^{+/-}$* was two mice for 1 week, four for 2 weeks, eight for 5 weeks, four for 8 weeks, and three for 6 months post-tamoxifen injections.

CagCreER;β-catenin$^{fl/fl}$ mice were generated by mating *β-catenin$^{fl/fl}$* mice with *CagCreER* mice that harbor a tamoxifen-inducible *Cre* (*CreER*) driven by the chick *β-actin* promoter/enhancer coupled to the cytomegarovirus immediate-early enhancer *STOCK Tg(CAG-cre/Esr1*)5Amc/J* from the Jackson Laboratory. *Col2CreER;Ext1$^{+/-}$* mice were generated by mating *Ext1$^{+/-}$* mice[17] and then mated with *Ext1 floxed* (*Ext1$^{fl/fl}$*) mice,[31] and the resulting littermates, *Col2CreER; Ext1$^{fl/-}$* and *Ext1$^{fl/-}$* received i.p. injections of tamoxifen (100 μg/10 μL per mouse) at day 5 and 7 after birth. *Col2CreER;Ext1$^{fl/fl}$* mice were also generated and received 100 μg/10 μL i.p. injections of tamoxifen per mouse at day 5 after birth. The mice were sacrificed 2 weeks after completion of the tamoxifen injections.

Histological, Histochemical, and Immunohistochemical Analyses

Knee joints were dissected, fixed with 4% (v/v) paraformaldehyde, decalcified with EDTA for 7 to 10 days, and

embedded in paraffin. Longitudinal sections of tibias and femurs (6 μm) were prepared and subjected to histological staining with H&E and safranin O and fast green. The sections were subjected to β-galactosidase (LacZ) activity staining using X-Gal Stock and Stain Base Solution (EMD Millipore Corporation, Billerica, MA), according to the manufacturer's protocol, and then counterstained with eosin. Proliferating activity was examined by detection of proliferating cell nuclear antigen (PCNA) using a PCNA staining kit (Life Technologies, Grand Island, NY) followed by counterstaining with methyl green. The PCNA staining results were observed under a Nikon Eclipse TE400 microscope (Nikon Instruments Inc., Melville, NY). SPOT Advanced software version 5.0 (Diagnostic Instruments Inc., Sterling Heights, MI) was used to capture and analyze images. The number of PCNA-positive cells and number of nuclei in three lateral and center regions of the growth plate were analyzed in two *β-catenin*$^{fl/fl}$ and two *Col2CreER;β-catenin*$^{fl/fl}$ mice. The ratio of the PCNA-positive cell number to the total cell number was calculated. Localization of collagen 10 was detected by immunohistochemical staining with an anti-collagen 10 antibody. Sections were treated with 0.1% pepsin in 0.02 N HCl for 10 minutes at 37°C, incubated with anti-collagen 10 antibody rabbit serum (1:1000; Cosmo Bio, Tokyo, Japan) in 10% goat serum in PBS for 1 hour at room temperature, followed by visualization of the antibody using the SuperPicture Polymer detection kit (Life Technologies) and counterstaining with methyl green. The sections that had been stained with nonimmune rabbit IgG (5 μg/mL; Vector Laboratories, Burlingame, CA) did not show specific staining.

To evaluate localization of osteoclasts, tartrate-resistant acid phosphatase (TRAP) staining was performed using a TRAP staining kit (Sigma-Aldrich, St. Louis, MO) by following the manufacturer's protocol.

The mouse growth plate paraffin sections were incubated with the rabbit polyclonal anti−β-catenin antibody (1:250; Cell Signaling Technology, Inc., Danvers, MA), followed by incubation with horseradish peroxidase conjugated anti-rabbit antibody (1:100; Vector Laboratories) and ImmPACT SG peroxidase substrate (Vector Laboratories) with methyl green counter staining.

Skeletal Analysis

Limb skeletons were analyzed by taking soft X-ray images using Bioptics piXarray100 (Core Medical Imaging, Inc., Kenmore, WA) using the automatic exposure mode. The knee joints and ribs were stained with alcian blue and alizarin red.

Chondrocyte Cultures

Chondrocytes were isolated from the epiphyseal cartilage from B6129SF2/J mice (Jackson Laboratory) at day 3 to 5 after birth. The epiphyseal cartilage pieces were digested with 0.05% trypsin in HBSS for 1 hour at 37°C and were then incubated with 86 U/mL collagenase type I (Worthington Biochemical Corporation, Lakewood, NJ) in serum-free Dulbecco's modified Eagle's medium overnight. The dissociated cells were plated on collagen 1 coated wells at the density of 30,000 cells per well in 96-well plates or 50,000 cells per well in 4-well culture slides (BD Biosciences, San Jose, CA) and cultured in Dulbecco's modified Eagle's medium containing 10% fetal bovine serum (Gemini Bio-Products, West Sacramento, CA). The cultures were incubated with 6BIO or Me-7BIO (Santa Cruz Biotechnology, Inc., Santa Cruz, CA) in the presence or absence of 3 mmol/L $CaCl_2$ and 6 mmol/L NaH_2PO_4 for 24 to 48 hours and subjected to a cell viability assay or terminal deoxynucleotidyl transferase-mediated dUTP

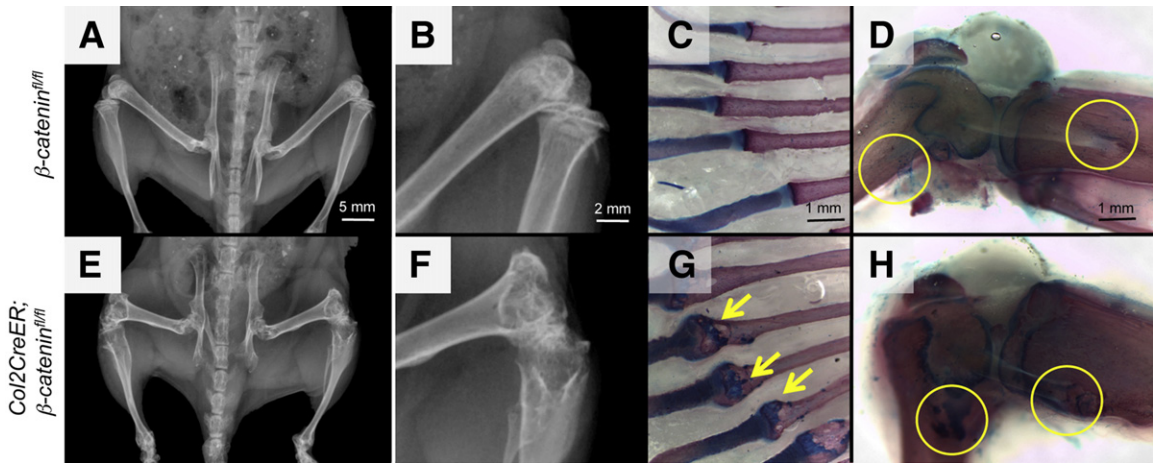

Figure 1 Structural deformity and ectopic cartilage formation in long bones and ribs in tamoxifen-injected *Col2CreER;β-catenin*$^{fl/fl}$ mice. *β-catenin*$^{fl/fl}$ mice (**A**–**D**) and their littermate *Col2CreER;β-catenin*$^{fl/fl}$ mice (**E**–**H**) received 100 μg/10 μL i.p. injections of tamoxifen per mouse at P5 to P7. Mice were sacrificed 5 weeks after completion of tamoxifen injections. Skeletal deformity and ectopic cartilage formation in knee joints (**A**, **B**, **D**–**F**, and **H**) and ribs (**C** and **G**) were examined by radiographical inspection (**A**, **B**, **E**, and **F**) and alcian blue/alizarin red skeletal staining (**C**, **D**, **G**, and **H**). **Arrows** indicate ectopic cartilage formation. **Circles** indicate regions of interest for ectopic cartilage formation in the knees.

nick-end labeling (TUNEL) assay. To examine cell viability, the cultures were incubated with 120 μg/mL 3-(4,5-dimethylthiazol-2-yl)−2,5-diphenyltetrazolium bromide (MTT, Life Technologies) in PBS for 1 hour at 37°C and then solubilized with 0.04N HCl in isopropanol. The absorbance was measured at 595 nm. The MTT (Life Technologies) substrate is converted to purple formazan by mitochondrial reductase. The conversion rate is used as a measure of viable cells. The cultures were also fixed with 3.7% neutralized formalin and subjected to a TUNEL assay using the ApopTag red *in situ* apoptosis detection kit (EMD Millipore Corporation) followed by DAPI nuclear staining.

Epiphyseal chondrocytes were also isolated from *Cag-CreER;β-catenin*$^{fl/fl}$ mice and the control *β-catenin*$^{fl/fl}$ littermates at days 3−5 after birth. The cultures were treated with 1 mmol/L 4-hydroxytamoxifen (Sigma-Aldrich) for 48 hours, followed by incubation without 4-hydroxytamoxifen for the additional 48 hours, harvested, and mixed with a collagen solution (3 mg/mL Cellmatrix; Nitta Gelatin Inc., Osaka, Japan) at the concentration of 6.0 to 8.0 × 10^6/mL by following the manufacturer's protocol. There was 250 μL per mouse cell mixture that was subcutaneously injected into athymic mice (CD-1 Nude Mouse; Charles River Laboratories International, Inc., Wilmington, MA). Transplants were collected 4 weeks later and subjected to histological inspection. The parallel cultures were harvested and subjected to immunoblot analysis to detect β-catenin and ERK using the anti−β-catenin antibody (1 μg/mL; BD Biosciences) and the anti-ERK antibody (1:1000; Cell Signaling Technology, Inc.).

To remove heparan sulfate proteoglycan, the chondrocytes isolated from B6129SF2/J mice were pre-treated with heparinase I from *Flavobacterium heparium* (Sigma-Aldrich) at 10 unit/mL for 16 hours and subjected to Top-flash reporter analysis[32] using a dual reporter kit (Promega, Madison WI).

Human Tissues

Paraffin sections of osteochondromas surgically removed from consenting HME patients, as well as rib cartilage removed during autopsy, were provided by the Pathology Core of the Children's Hospital of Philadelphia. The slides we used in this study had been made for clinical diagnosis, but were no longer needed and were completely de-identified before being provided for the present study. The study was determined to be nonhuman subjects' research by The Children's Hospital of Philadephia Research Institute's Institutional Review Board.

The sections were treated with 0.1% pepsin in 0.02 N HCl for 10 minutes at 37°C after deparaffinization, blocked with 10% goat serum in PBS for 1 hour, and incubated with the anti−β-catenin mouse antibody (1 μg/mL, BD Biosciences) or nonimmune mouse IgG (1 μg/mL, Vector Laboratories) at 4°C overnight. The sections were then incubated with Alexa Fluor 594-labeled anti-mouse IgG (1 μg/mL) for 1 hour at room temperature followed by DAPI staining for nuclei. The images were taken with a Nikon Eclipse TE2000-U fluorescent microscope (Nikon Instruments Inc.). ImagePro software version 5.0 (Media Cybermetics, Inc., Rockville, MD) was used to capture and analyze images of 5 to 7 fields per sample (seven osteochondromas and four rib cartilages). The β-catenin images were first processed by subtraction of the background staining intensity that had been obtained from the samples stained with the nonimmune IgG. The number of β-catenin positive cells and DAPI-positive cells were counted, and the ratio of the β-catenin positive cell number to the DAPI-positive cell number was calculated.

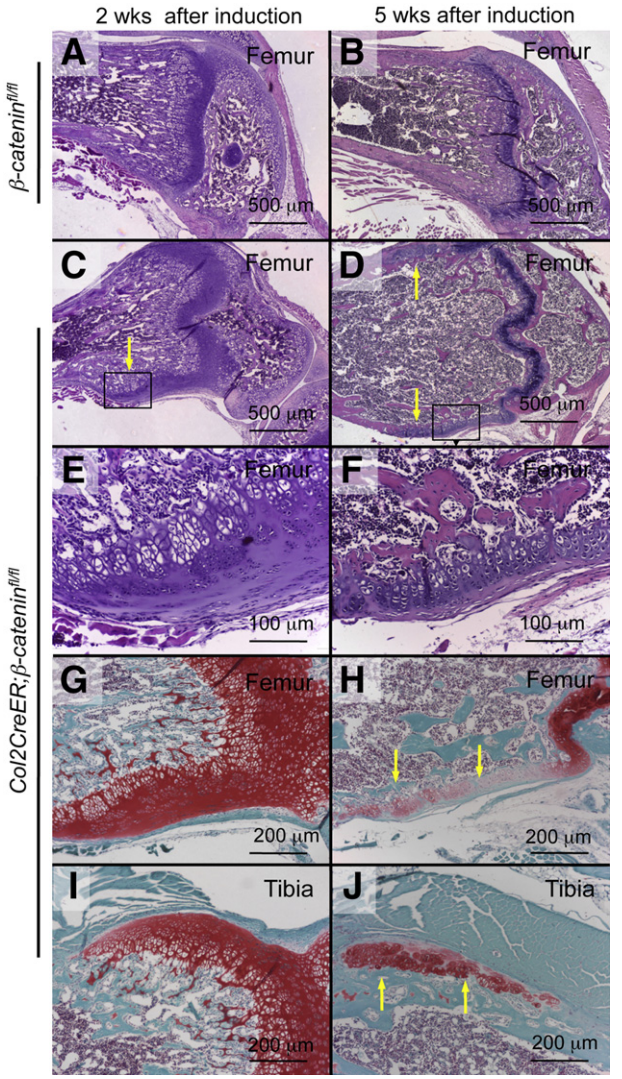

Figure 2 Outgrowth of growth plate and ectopic cartilage in periosteum in tamoxifen-injected *Col2CreER;β-catenin*$^{fl/fl}$ mice. *Col2CreER;β-catenin*$^{fl/fl}$ mice (**C**—**J**) and their littermate *β-catenin*$^{fl/fl}$ mice (**A** and **B**) received 100 μg/10 μL i.p. injections of tamoxifen per mouse at P5 to P7. Longitudinal sections of knee joints were prepared at 2 weeks (**A**, **C**, **E**, **G**, and **I**) or 5 weeks (**B**, **D**, **F**, **H**, and **J**) after completion of the tamoxifen injections. **Arrows** indicate out-growing growth plate (**C**) or ectopic cartilage masses embedded in the periosteum (**D**, **H**, and **J**). **Boxed areas** in **C** and **D** are enlarged in **E** and **F**, respectively.

Statistical Methods

Results were analyzed using InStat 3 version 3.1a (GraphPad Software, Inc., La Jolla, CA). A one-way analysis of variance with a Tukey-Kramer Multiple Comparison Test was used to identify the differences. The threshold for significance for all tests was set as $P < 0.05$.

Results

Formation of Multiple Ectopic Cartilaginous Masses in Tamoxifen-Treated *Col2CreER;β-catenin$^{fl/fl}$* Mice

Col2CreER;β-catenin$^{fl/fl}$ and control *β-catenin$^{fl/fl}$* mice received tamoxifen injection at days 5, 6 and 7 or days 5 and 7 after birth to conditionally ablate the *β-catenin* gene and were kept until 5 weeks after completion of tamoxifen injections. X-ray analysis revealed that the femur and tibia of tamoxifen-injected *Col2CreER;β-catenin$^{fl/fl}$* mice had become severely deformed (Figure 1, E and F), whereas, the corresponding skeletal elements in control tamoxifen-injected *β-catenin$^{fl/fl}$* mice showed no obvious abnormality (Figure 1, A and B). The knee joints and ribs were harvested and stained with alcian blue and alizarin red to inspect skeletal deformity and possible formation of ectopic cartilage. The costochondral junctions of ribs in the tamoxifen-injected *Col2CreER;β-catenin$^{fl/fl}$* mice were swollen (Figure 1G) and displayed ectopic cartilaginous masses that were positive for alcian blue staining (Figure 1G). In contrast, ribs in the tamoxifen-injected control mice were normal (Figure 1C). Ectopic cartilaginous masses were also detected in tibias and femurs of the tamoxifen-injected *Col2CreER;β-catenin$^{fl/fl}$* mice (Figure 1H), but not in the controls (Figure 1D). Similar outcomes were seen using the other *Col2CreER* (*DC*) mouse line. The *Col2CreER;β-catenin$^{fl/fl}$* mice that had not received a tamoxifen injection did not show any significant skeletal abnormality (data not shown).

To examine the histology of ectopic cartilaginous masses, we prepared longitudinal sections of knee joints that had been harvested from the tamoxifen-injected *Col2CreER;β-catenin$^{fl/fl}$* or the control *β-catenin$^{fl/fl}$* mice at 2 (Figure 2, A, C, E, G, and I) or 5 weeks (Figure 2, B, D, F, H, and J) after completion of the tamoxifen injections. The ectopic masses were present along the lateral side of the tibia and femur growth plates in the direction of the metaphysis in the injected *Col2CreER;β-catenin$^{fl/fl}$* mice at 2 weeks after the tamoxifen injections (Figure 2C), and were present in both the distal femur and proximal tibia (Figure 2, C, E, and G). Growth plates of the control *β-catenin$^{fl/fl}$* mice were normal (Figure 2A). Five weeks after the tamoxifen injections, the ectopic cartilaginous masses were embedded in the periosteum (Figure 2, D, F, H, and J). They retained a columnar structure, but did not contain typical hypertrophic cells (Figure 2F). Both mutant femur and tibia showed decreased bone volume (Figure 2D) compared to the controls (Figure 2B), as previously reported.[24] Some ectopic cartilaginous masses were disconnected from the growth plate (Figure 2J). Interestingly, the ectopic masses showed similarities to those in the *Ext* mutant mice, which have been reported as osteochondroma animal models.[17–19] Indeed, we confirmed that conditional *Ext1* ablation caused formation of similar outgrowths near the growth plates at early time points after gene ablation was induced (Supplemental Figure S1). In addition, β-catenin immunostaining revealed that the growth plate of *Col2CreER;Ext1$^{fl/fl}$* mice injected with tamoxifen at P5 (100 μg/10 μL per mouse)

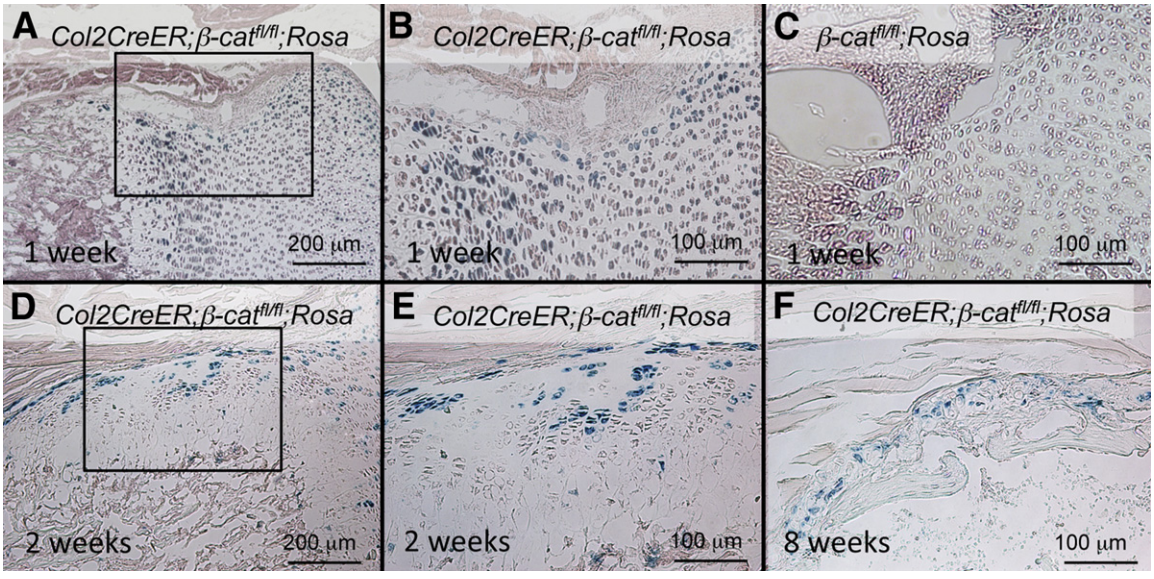

Figure 3 Localization of Cre-positive cells after tamoxifen injection in *Col2CreER;β-catenin$^{fl/fl}$;Rosa-LacZ* mice. *Col2CreER;β-catenin$^{fl/fl}$;Rosa-LacZ* mice (**A**, **B**, and **D**–**F**) and littermate *β-catenin$^{fl/fl}$;Rosa-LacZ* mice (**C**) received 100 μg/10 μL i.p. injections of tamoxifen per mouse at P5 and P7. Longitudinal sections of knee joints were prepared at 1 (**A**–**C**), 2 (**D** and **E**), or 8 (**F**) weeks after completion of the tamoxifen injections and subjected to β-galactosidase staining. **B** and **E**: Magnified images of the **boxed areas** in **A** and **D**, respectively.

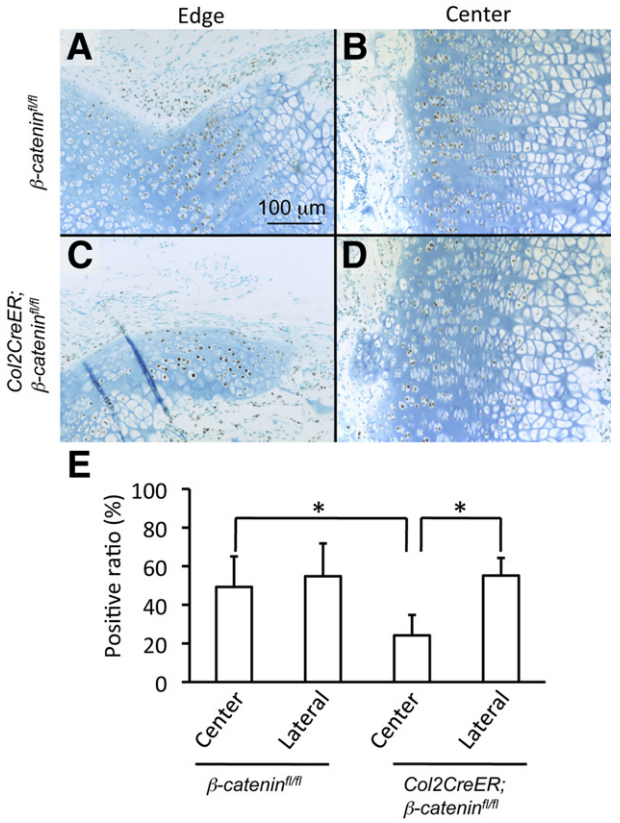

Figure 4 Imbalance of cell proliferating activity in growth plate in the tamoxifen injected *Col2CreER;β-catenin*$^{fl/fl}$mice. *Col2CreER;β-catenin*$^{fl/fl}$*;Rosa-LacZ* mice (**A** and **B**) and littermate *β-catenin*$^{fl/fl}$*;Rosa-LacZ* mice (**C** and **D**) received 100 μg/10 μL i.p. injections of tamoxifen per mouse at P5 and P7. Longitudinal sections of knee joints were prepared at 2 weeks after completion of the tamoxifen injections and subjected to PCNA staining. **E:** Ratios of PCNA-positive cells were measured (see *Materials and Methods*). *$P < 0.05$

showed much weaker staining, especially in the hypertrophic zone (Supplemental Figure S1F), suggesting that *Ext1*-deficient chondrocytes had weaker β-catenin signaling activity. In good agreement, heparinase-treated chondrocytes in culture displayed reduced responsiveness to Wnt3a treatment compared to control cells (Supplemental Figure S1G).

Characterization of β-Catenin-Deficient Chondrocytes

Next, we generated *Col2CreER;β-catenin*$^{fl/fl}$ mice in *R26Rosa-lox-stop-lox-LacZ* background and examined where the Cre activity was induced and how the Cre-sensitive cells contributed to ectopic cartilage formation by monitoring Cre-induced LacZ activity. One week after completion of the tamoxifen injections, a large number of LacZ positive cells were present in the entire cartilage, but hardly any were present in the perichondrium and periosteum (Figure 3, A and B), indicating that the induction of Cre activity is largely limited to cartilage. The control tamoxifen-injected *β-catenin*$^{fl/fl}$*;Rosa-LacZ*$^{+/-}$ mice essentially displayed no LacZ-positive cells (Figure 3C). The ectopic cartilaginous masses present at 2 weeks after the tamoxifen injections were composed of both LacZ-positive and negative cells, and the hypertrophic cells in the outgrowing lesions were mostly negative (Figure 3, D and E). Eight weeks after the last tamoxifen injection, the ectopic cartilage masses did not contain enlarged hypertrophic cells and were largely composed of LacZ-positive cells (Figure 3F). These findings suggest that the β-catenin-deficient cells autonomously form the ectopic cartilage masses and could originate from the growth plate.

PCNA staining was performed to examine cell proliferating activity. The PCNA-positive cells were evenly located

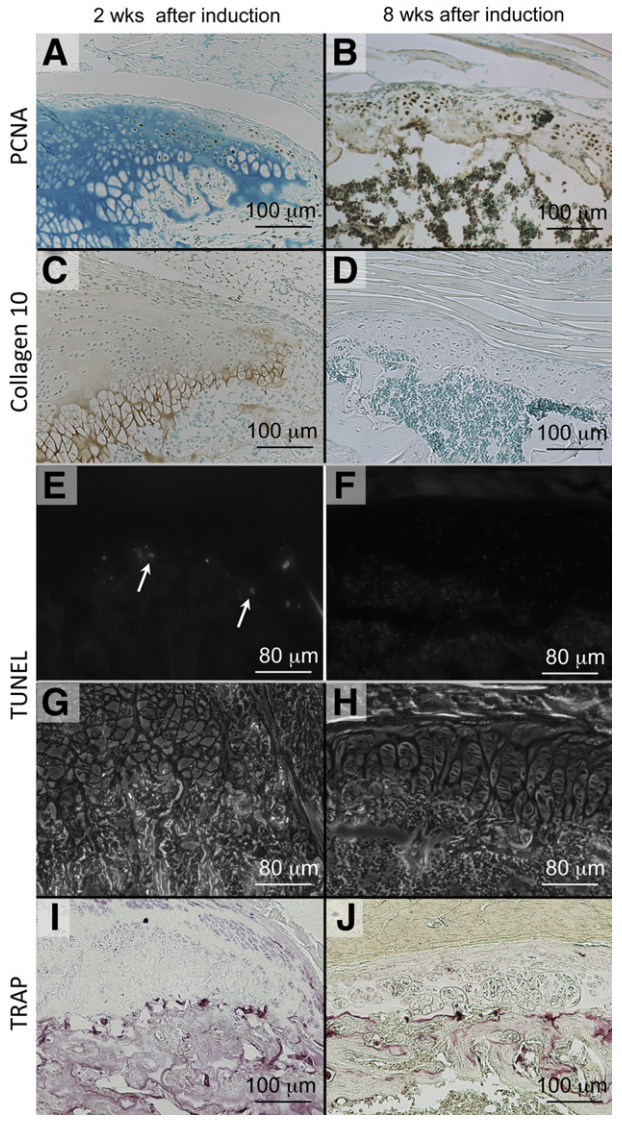

Figure 5 PCNA, collagen 10, TUNEL, and TRAP staining in ectopic cartilaginous masses at early and late stages after tamoxifen injections. *Col2CreER;β-catenin*$^{fl/fl}$*;Rosa-LacZ* mice received 100 μg/10 μL i.p. injections of tamoxifen per mouse at P5 and P7. Longitudinal sections of knee joints were prepared at 2 weeks (**A**, **C**, **E**, **G**, and **I**) or 8 weeks (**B**, **D**, **F**, **H**, and **J**) after completion of the tamoxifen injections and subjected to PCNA (**A** and **B**), collagen 10 immunostaining (**C** and **D**), TUNEL (**E** and **F**), and TRAP (**I** and **J**) staining. The arrows in **E** indicates apoptotic cells. **G** and **H**: Phase contrast images (**E** and **F**), respectively.

along the edge and center of the growth plate in the tamoxifen-injected control mice (Figure 4, A and B). In contrast, PCNA-positive cells were abnormally distributed in the growth plate in tamoxifen-injected *Col2CreER;β-catenin*$^{fl/fl}$ mice. The number of labeled cells was lower in the center (Figure 4D) as compared with the outgrowing lesion (Figure 4C). A semiquantitative analysis supported this observation (Figure 4E), indicating that the chondrocytes in the center of the growth plate in β-catenin deficient mice exhibited lower proliferating activity that those in the outgrowths.

Then we compared the ectopic cartilaginous masses at the initial and later stages. The outgrowing masses at 2 weeks after the tamoxifen injections showed phenotypic characteristics similar to those of the normal growth plates, including collagen 10 expression in the hypertrophic zone (Figure 5C), presence of apoptotic cells (Figure 5, E and G), and TRAP-positive osteoclasts (Figure 5I) under the hypertrophic zone. There were no significant changes in expression levels of collagen 10 and the number of apoptotic cells and TRAP-positive cells in control versus β-catenin-deficient growth plates, although the latter were structurally overgrowing. At the later stages, the majority of cells in the ectopic masses were still positive for PCNA (Figure 5B). Collagen 10-producing cells (Figure 5D) and apoptotic cells were not found (Figure 5, F and H), although TRAP-positive cells were detected adjacent to the ectopic cartilage (Figure 5J). These findings indicate that the ectopic chondrocytes retained their proliferating activity and did not undergo hypertrophy and apoptosis.

The ectopic cartilaginous masses were still present at 6 months after the tamoxifen injections. The cartilaginous masses gradually increased in volume, bulging into adjacent skeletal muscles (Supplemental Figure S2A). Microscopy of these lesions showed proliferating chondrocytes, cytological atypia, including bi-nucleated cells (arrows), and prominent vascularity reminiscent of capillary ingrowth (Supplemental Figure S2B). Disorganization of tissues and the appearance of atypical cells in the cartilaginous masses were observed in each of three separate samples (Supplemental Figure S2, B–D).

The previously described data indicated that loss of β-catenin rendered chondrocytes more resistant to bone replacement in the process of endochondral ossification. To test this possibility more directly, we isolated chondrocytes from the compound mice (*CagCreER;β-catenin*$^{fl/fl}$) harboring *floxed β-catenin* and a tamoxifen-inducible *Cre* (*CreER*) driven by the chick *β-actin* promoter/enhancer coupled to the cytomegalovirus immediate-early enhancer (*CagCreER*). The chondrocytes from *CagCreER;β-catenin*$^{fl/fl}$ and *β-catenin*$^{fl/fl}$ mouse cartilage were treated with 1 μmol/L 4-hydroxytamoxifen for 2 days; immunoblot analysis confirmed that the former contained no detectable β-catenin, whereas the control cells did (Figure 6D). Both populations were transplanted subcutaneously into athymic mice. The control chondrocyte transplants were completely replaced by bone and fatty marrow by 4 weeks (Figure 6A), whereas the tissue formed by *β-catenin*-deficient chondrocytes showed resistance to bone replacement and persisted as a cartilaginous mass (Figure 6B) comprising heterogeneous cells (Figure 6C).

To further examine the normal roles of β-catenin signaling on cell apoptosis, we treated normal chondrocytes with 6BIO, a stimulator of the Wnt/β-catenin signaling pathway. Treatment with 6BIO changed the cell morphology, and many cells were shrunken and had irregular cell membranes (Figure 7B). TUNEL staining revealed that

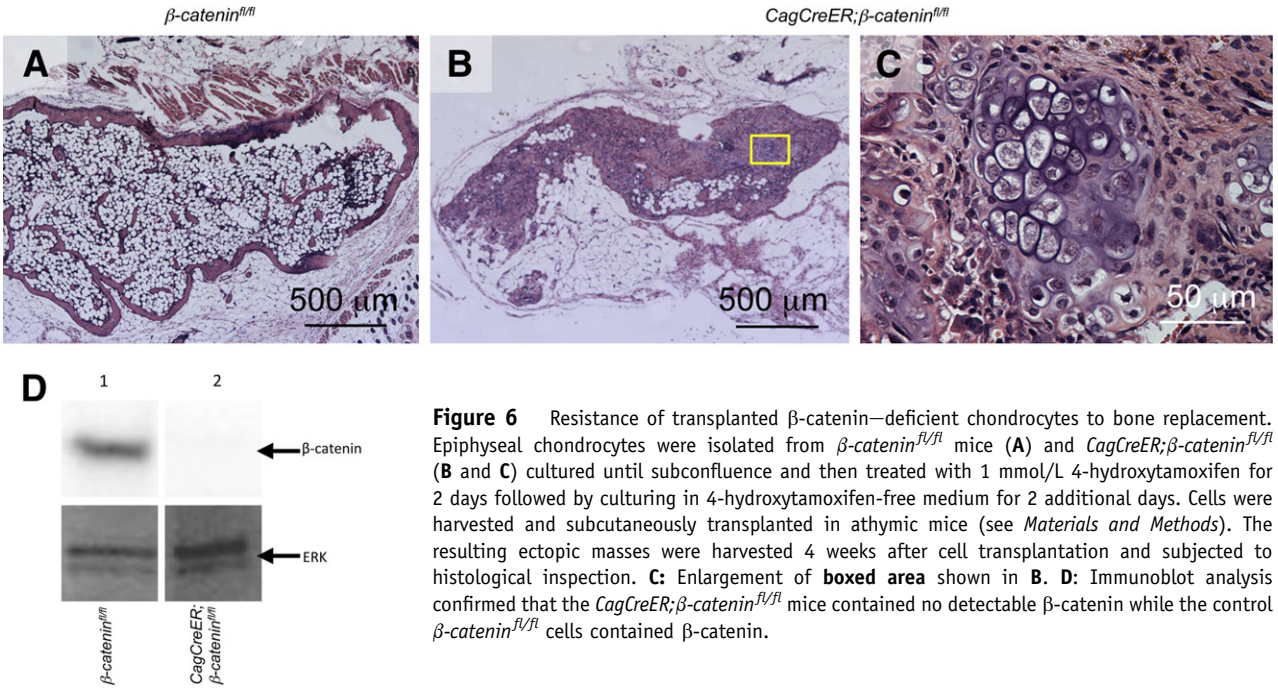

Figure 6 Resistance of transplanted β-catenin–deficient chondrocytes to bone replacement. Epiphyseal chondrocytes were isolated from *β-catenin*$^{fl/fl}$ mice (**A**) and *CagCreER;β-catenin*$^{fl/fl}$ (**B** and **C**) cultured until subconfluence and then treated with 1 mmol/L 4-hydroxytamoxifen for 2 days followed by culturing in 4-hydroxytamoxifen-free medium for 2 additional days. Cells were harvested and subcutaneously transplanted in athymic mice (see *Materials and Methods*). The resulting ectopic masses were harvested 4 weeks after cell transplantation and subjected to histological inspection. **C:** Enlargement of **boxed area** shown in **B**. **D**: Immunoblot analysis confirmed that the *CagCreER;β-catenin*$^{fl/fl}$ mice contained no detectable β-catenin while the control *β-catenin*$^{fl/fl}$ cells contained β-catenin.

the 6BIO-treated cultures contained many apoptotic cells (Figure 7E). A cell viability assay showed that 6BIO had impaired cell survival in a dose-dependent manner (Figure 7G), whereas treatment with a control inactive reagent, Me-7BIO, did not induce any appreciable changes in the previously described parameters (Figure 7, C, F, and G), as also seen in the cultures receiving the vehicle (dimethyl sulfoxide) (Figure 7, A, D, and G). Furthermore, 6BIO treatment enhanced the apoptotic effects of high doses of calcium and phosphate ions known to cause apoptosis in growth plate chondrocytes[33,34] (Figure 7G).

β-Catenin in Human Osteochondromas and Growth Plates

Osteochondromas typically contain a cartilage cap and underlying bone. Surgically retrieved cartilage caps from HME patients and rib growth plate sections from fetal autopsies were subjected to immunohistochemical analysis of β-catenin. We divided the cartilage caps into two regions (Supplemental Figure S3A): a surface region generally consisting of single cells (Figure 8I) and a deeper part located closer to the bone consisting of relatively large cells (Figure 8J). We only observed relatively weak β-catenin staining in some of the solitary cells and large cells (Figure 8, A, B, E, and F). The resting zone and hypertrophic zone in the control growth plates were separately inspected (Supplemental Figure S3B). The degree of β-catenin staining was very low in the resting zone (Figure 8, C and G), but fairly high in the hypertrophic zone (Figure 8, D and H). The number of β-catenin–positive cells in the cartilage caps was comparable to that seen in the resting zone but was much lower than that in the hypertrophic zone (Figure 8M), suggesting that cartilage

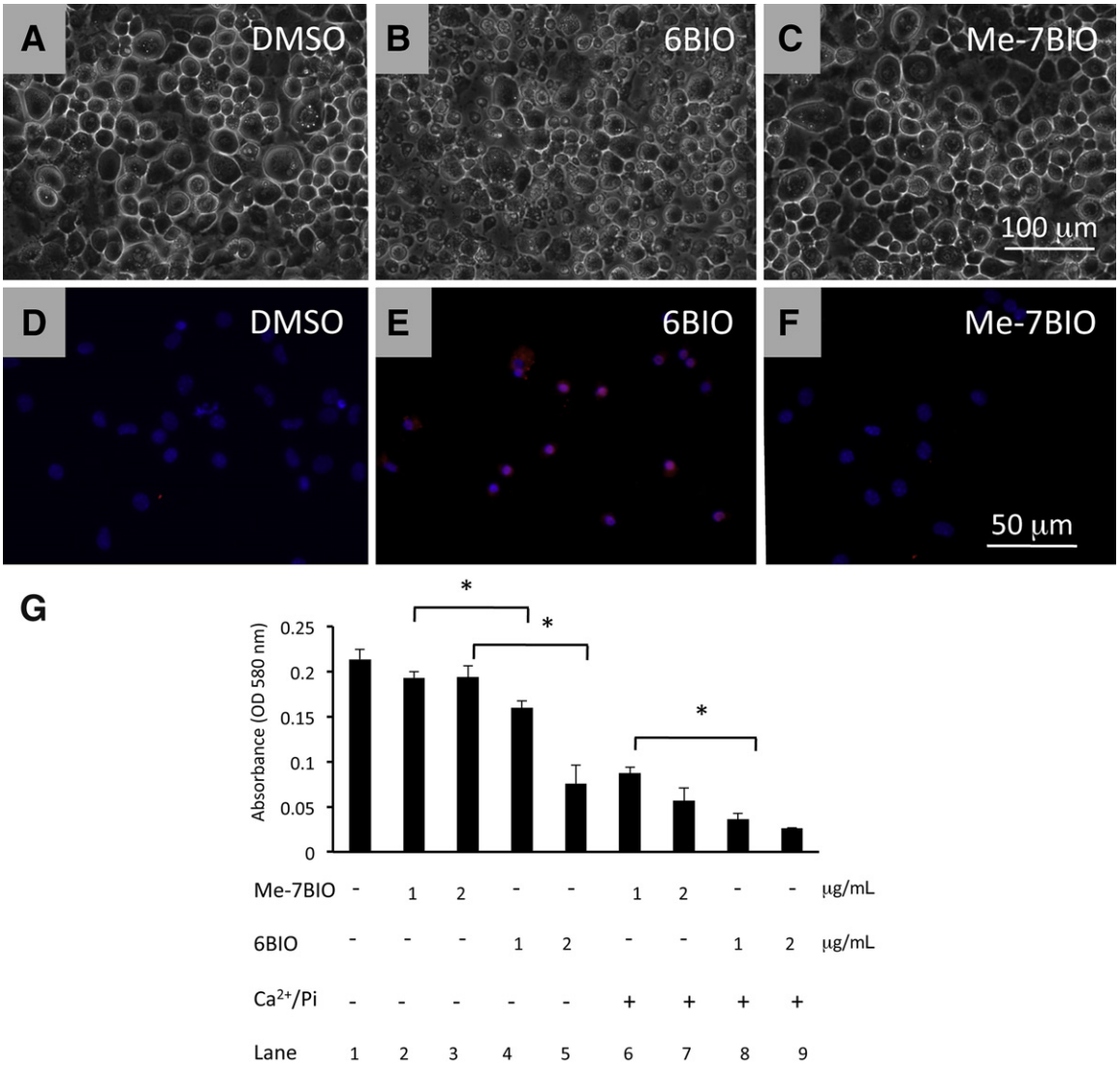

Figure 7 Stimulation of cell apoptosis and cell death in chondrocytes by 6BIO treatment. **A**–**F**: Epiphyseal chondrocytes isolated from B6129SF2/J mice were treated with 2 μg/mL 6BIO (**B**), 2 μg/mL Me-7BIO (**C**), or vehicle (**A**) dimethyl sulfoxide for 24 hours and subjected to TUNEL staining (**D**–**F**) after photographic images were taken (**A**–**C**). **G**: Cells were treated with 6BIO, Me-7BIO, or vehicle in the presence or absence of 3 mmol/L $CaCl_2$ and 6 mmol/L NaH_2PO_4 (Ca^{2+}/Pi) for 24 hours and were subjected to a cell viability assay. *$P < 0.05$.

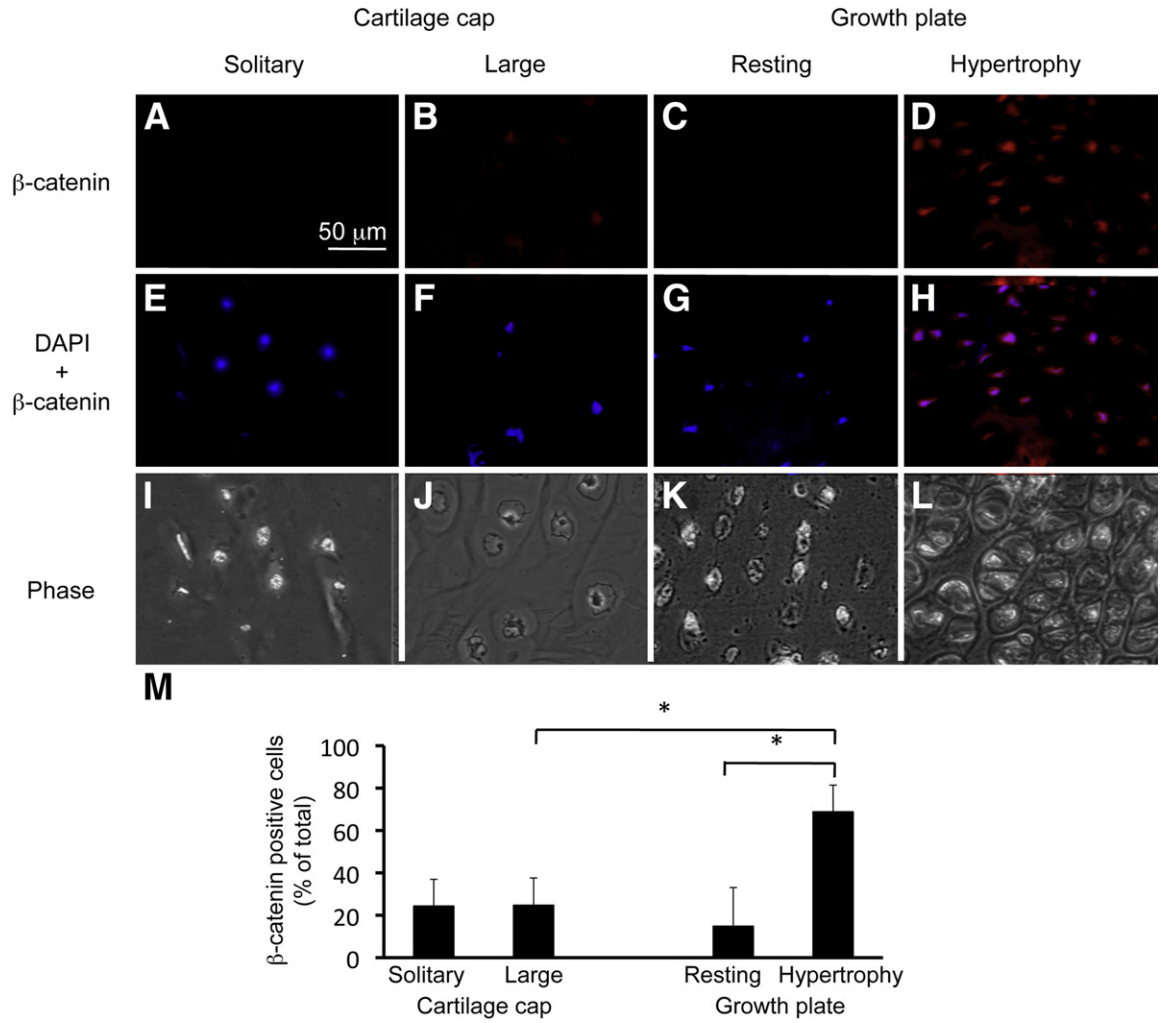

Figure 8 Immunolocalization of β-catenin in ostechondromas and rib growth plates. **A**–**L**: Sections of osteochondromas from HME patients (**A**, **B**, **E**, **F**, **I**, and **J**) and rib growth plate obtained from autopsy (**C**, **D**, **G**, **H**, **K**, and **L**) were subjected to immunofluorescence staining for β-catenin. Cartilage caps of osteochondromas were divided into two parts: a region composing of solitary and relatively small cells (Solitary), and a region adjacent to the bone and composed of relatively large cells (Large). Resting zone (Resting) and hypertrophic zone (Hypertrophy) of growth plates were separately inspected. **A**–**D**: β-catenin staining; (**E**–**H**) merged images of β-catenin staining (red) and DAPI nuclear staining (blue); (**I**–**L**) phase contrast images (**A**–**D**), respectively. **M**: Ratios of β-catenin positive cells were evaluated as previously described (see *Materials and Methods*). $*P < 0.05$.

caps in osteochondromas in HME patients have lower β-catenin signaling activity than that present in normal growth plates.

Discussion

Mechanisms of Ectopic Chondroma-Like Mass Formation in the β-Catenin Deficient Mice

We demonstrate here that postnatal conditional ablation of β-catenin induces formation of periosteal cartilage masses in mice. Our data relate well with those in previous studies showing that loss of β-catenin can induce ectopic cartilage formation during embryogenesis.[26,27] These reports have also indicated that β-catenin signaling is required for osteoblast differentiation of mesenchymal cells and that the absence of β-catenin induces mesenchymal cell differentiation into chondrocytes. In our mouse models, Cre-recombinase activity was largely limited to cartilage and was essentially undetectable in noncartilaginous tissues, including perichondrium and periosteum. The data suggest that ectopic cartilage originates via abnormal expansion of the growth plate into the lateral site of perichondrium and is eventually embedded within the periosteum with time. It is therefore likely that ectopic cartilage formation is largely induced by abnormal behavior and function of growth plate chondrocytes in our models. However, we cannot exclude the possibility that neodifferentiation of perichondrium or periosteum-associated skeletal progenitor cells into chondrocytes may also contribute to ectopic cartilage formation.

Our data offers insights into possible mechanisms by which cartilage outgrowths form. One possibility is suggested by the apparent differences in chondrocyte proliferation in the central versus peripheral portions of mutant growth plates. The rates appear to be higher in the lateral part than in the

center growth plate revealed by PCNA staining. This imbalance of cell proliferating activity could derange coordinated longitudinal expansion of the growth plate and lead to lateral overgrowth. In addition, the perichondrium flanking the outgrowing growth plate in the tamoxifen-injected mutant mice appears thinner than that in the control growth plate. Such alteration could decrease the mechanical strength of the perichondrium, resulting in deformation and outgrowth of the growth plate. The outgrowing growth plate initially contained hypertrophic cells positive for collagen 10 and apoptotic cells at the base. These cells had not activated Cre-recombinase, as determined by β-galactosidase activity in *Col2CreER;β-catenin$^{fl/fl}$* mice in *Rosa-LacZ* background. In contrast, the ectopic cartilaginous masses embedded in the periosteum at later stages did not contain collagen 10 positive cells and apoptotic cells, and most of the cells were β-galactosidase-positive and likely β-catenin-deficient. Furthermore, transplants of β-catenin-deficient chondrocytes into athymic mice were not replaced by bone and remained cartilaginous for long periods of time. Wnt/β-catenin signaling has been demonstrated to stimulate cell proliferation and survival in various types of cells, especially in cancer cells.[35,36] However, activation of this signaling stimulates apoptosis, as well as proliferation in intestinal epithelial cells *in vivo*[37] and also controls frequency of apoptosis in hematopoietic stem/progenitor cells through suppressing Bcl2 expression.[38] Furthermore, overexpression of β-catenin causes cell death independently of its transactivation function.[39] Thus β-catenin could regulate apoptosis in chondrocytes through multiple mechanisms and contexts.

Taken together, our data indicate that hypertrophic cells within the outgrowing lesion did not undergo ablation of the β-catenin gene, but were brought along by the β-catenin-deficient chondrocytes during deformation of the growth plate, proceeded toward the endochondral bone formation process, and were replaced by bone while the β-catenin-deficient cells remained as cartilaginous masses within the periosteum. Thus, the process of ectopic chondroma-like mass formation in our mouse model can be divided into two stages. Loss of β-catenin in the growth plate would initially induce a deformity of the growth plate resulting in lateral outgrowth of the growth plate itself. Subsequently, the β-catenin deficient chondrocytes would resist hypertrophy and apoptosis and would give rise to long-lasting ectopic cartilaginous masses persisting within the periosteum.

β-Catenin Signaling in Chondroma Formation

Recent studies have suggested that dysregulation of hedgehog and fibroblast growth factor signaling results in osteochondroma formation under conditions of deficiency of *EXT* expression and heparan sulfate production in HME patients.[5,13] In the present study, we observed similarities in the formation of ectopic chondroma-like masses in between our β-catenin-deficient mice and the *Ext* mutant mice previously reported to represent HME osteochondroma models.[17–19] The topography and histology of ectopic cartilaginous masses forming in our mouse models show features similar to those in Ext mutants[17–19] in that they both form adjacent to the growth plate in ribs, distal tibiae, and proximal femurs, and they exhibit growth-plate like structures, and persist in the periosteum over time. Similar outgrowths of the growth plate were observed in two different types of mutant mice.[18,19] However, the deficiency of β-catenin resulted in more severe skeletal deformity as compared to those in *Ext* mutants, indicating that β-catenin-deficient mice may have additional pathological complications. We also demonstrate here that the cartilage caps present in HME patient osteochondromas contained a much lower number of β-catenin-positive cells as compared to hypertrophic chondrocytes of the normal growth plate. These findings suggest that loss or decrease in β-catenin signaling could be a novel pathway involved in the pathogenesis of osteochondroma formation in HME. Genetic and molecular interactions between the Wnt signaling pathway and heparan sulfate proteoglycans have been demonstrated in Drosophila and vertebrates.[40–44] Furthermore, previous studies have indicated that heparan sulfate proteoglycans stabilize Wnt proteins and modulate Wnt signaling activities negatively or positively.[41,43,45–47] Our *in vivo* and *in vitro* results are consistent with these reports. Thus, a deficiency in heparan sulfate may decrease Wnt/β-catenin signaling, which in turn could contribute to long-term persistence of cartilage caps in osteochondromas.

Acknowledgments

We thank Dr. Susan Mackem (National Cancer Institute) for providing *Col2CreER;β-catenin$^{fl/fl}$* mice and Aisha Hargget, Diane Pilchak, Christine Macolino, and Wei-en Tung for their technical assistance.

Supplemental Data

Supplemental material for this article can be found at *http://dx.doi.org/10.1016/j.ajpath.2012.11.012*.

References

1. Unni KK, Inwards CY, Bridge JA, Kindblom L-G, Wold LE: Osteochondroma. Edited by Silverberg SG. Tumors of the bones and joints. Washington, American Registry of Pathology, 2005, pp 37–46
2. Unni KK, Inwards CY, Bridge JA, Kindblom L-G, Wold LE: Enchondromas. Tumors of the bones and joints. Washington, American Registry of Pathology, 2005. pp 46–52
3. Marco RA, Gitelis S, Brebach GT, Healey JH: Cartilage tumors: evaluation and treatment. J Am Acad Orthop Surg 2000, 8:292–304
4. Pannier S, Legeai-Mallet L: Hereditary multiple exostoses and enchondromatosis. Best Pract Res Clin Rheumatol 2008, 22:45–54
5. Bovee JV, Hogendoorn PC, Wunder JS, Alman BA: Cartilage tumours and bone development: molecular pathology and possible therapeutic targets. Nat Rev Cancer 2010, 10:481–488
6. Gelderblom H, Hogendoorn PC, Dijkstra SD, van Rijswijk CS, Krol AD, Taminiau AH, Bovee JV: The clinical approach towards chondrosarcoma. Oncologist 2008, 13:320–329
7. de Andrea CE, Hogendoorn PC: Epiphyseal growth plate and secondary peripheral chondrosarcoma: the neighbours matter. J Pathol 2012, 226:219–228

8. Riedel RF, Larrier N, Dodd L, Kirsch D, Martinez S, Brigman BE: The clinical management of chondrosarcoma. Curr Treat Options Oncol 2009, 10:94−106
9. Healey JH, Lane JM: Chondrosarcoma. Clin Orthop Relat Res 1986, 204:119−129
10. Hopyan S, Gokgoz N, Poon R, Gensure RC, Yu C, Cole WG, Bell RS, Juppner H, Andrulis IL, Wunder JS, Alman BA: A mutant PTH/PTHrP type I receptor in enchondromatosis. Nat Genet 2002, 30: 306−310
11. Rozeman LB, Sangiorgi L, Briaire-de Bruijn IH, Mainil-Varlet P, Bertoni F, Cleton-Jansen AM, Hogendoorn PC, Bovee JV: Enchondromatosis (Ollier disease, Maffucci syndrome) is not caused by the PTHR1 mutation p.R150C. Hum Mutat 2004, 24:466−473
12. Rozeman LB, Hameetman L, Cleton-Jansen AM, Taminiau AH, Hogendoorn PC, Bovee JV: Absence of IHH and retention of PTHrP signalling in enchondromas and central chondrosarcomas. J Pathol 2005, 205:476−482
13. Zak BM, Crawford BE, Esko JD: Hereditary multiple exostoses and heparan sulfate polymerization. Biochim Biophys Acta 2002, 1573: 346−355
14. Lin X: Functions of heparan sulfate proteoglycans in cell signaling during development. Development 2004, 131:6009−6021
15. Ballock RT, O'Keefe RJ: Physiology and pathophysiology of the growth plate. Birth Defects Res C Embryo Today 2003, 69: 123−143
16. de Crombrugghe B, Lefebvre V, Nakashima K: Regulatory mechanisms in the pathways of cartilage and bone formation. Curr Opin Cell Biol 2001, 13:721−727
17. Zak BM, Schuksz M, Koyama E, Mundy C, Wells DE, Yamaguchi Y, Pacifici M, Esko JD: Compound heterozygous loss of Ext1 and Ext2 is sufficient for formation of multiple exostoses in mouse ribs and long bones. Bone 2011, 48:979−987
18. Jones KB, Piombo V, Searby C, Kurriger G, Yang B, Grabellus F, Roughley PJ, Morcuende JA, Buckwalter JA, Capecchi MR, Vortkamp A, Sheffield VC: A mouse model of osteochondromagenesis from clonal inactivation of Ext1 in chondrocytes. Proc Natl Acad Sci USA 2010, 107:2054−2059
19. Matsumoto K, Irie F, Mackem S, Yamaguchi Y: A mouse model of chondrocyte-specific somatic mutation reveals a role for Ext1 loss of heterozygosity in multiple hereditary exostoses. Proc Natl Acad Sci USA 2010, 107:10932−10937
20. Hartmann C: Skeletal development−Wnts are in control. Mol Cells 2007, 24:177−184
21. Day TF, Yang Y: Wnt and hedgehog signaling pathways in bone development. J Bone Joint Surg Am 2008, 90(Suppl 1):19−24
22. Church VL, Francis-West P: Wnt signalling during limb development. Int J Dev Biol 2002, 46:927−936
23. Koyama E, Shibukawa Y, Nagayama M, Sugito H, Young B, Yuasa T, Okabe T, Ochiai T, Kamiya N, Rountree RB, Kingsley DM, Iwamoto M, Enomoto-Iwamoto M, Pacifici M: A distinct cohort of progenitor cells participates in synovial joint and articular cartilage formation during mouse limb skeletogenesis. Dev Biol 2008, 316:62−73
24. Yuasa T, Kondo N, Yasuhara R, Shimono K, Mackem S, Pacifici M, Iwamoto M, Enomoto-Iwamoto M: Transient activation of Wnt/[beta]-catenin signaling induces abnormal growth plate closure and articular cartilage thickening in postnatal mice. Am J Pathol 2009, 175: 1993−2003
25. Hu H, Hilton MJ, Tu X, Yu K, Ornitz DM, Long F: Sequential roles of Hedgehog and Wnt signaling in osteoblast development. Development 2005, 132:49−60
26. Hill TP, Spater D, Taketo MM, Birchmeier W, Hartmann C: Canonical Wnt/beta-catenin signaling prevents osteoblasts from differentiating into chondrocytes. Dev Cell 2005, 8:727−738
27. Day TF, Guo X, Garrett-Beal L, Yang Y: Wnt/beta-catenin signaling in mesenchymal progenitors controls osteoblast and chondrocyte differentiation during vertebrate skeletogenesis. Dev Cell 2005, 8: 739−750
28. Enomoto-Iwamoto M, Kitagaki J, Koyama E, Tamamura Y, Wu C, Kanatani N, Koike T, Okada H, Komori T, Yoneda T, Church V, Francis-West PH, Kurisu K, Nohno T, Pacifici M, Iwamoto M: The Wnt antagonist Frzb-1 regulates chondrocyte maturation and long bone development during limb skeletogenesis. Dev Biol 2002, 251:142−156
29. Nakamura E, Nguyen MT, Mackem S: Kinetics of tamoxifen-regulated Cre activity in mice using a cartilage-specific CreER(T) to assay temporal activity windows along the proximodistal limb skeleton. Dev Dyn 2006, 235:2603−2612
30. Chen M, Lichtler AC, Sheu TJ, Xie C, Zhang X, O'Keefe RJ, Chen D: Generation of a transgenic mouse model with chondrocyte-specific and tamoxifen-inducible expression of Cre recombinase. Genesis 2007, 45: 44−50
31. Inatani M, Irie F, Plump AS, Tessier-Lavigne M, Yamaguchi Y: Mammalian brain morphogenesis and midline axon guidance require heparan sulfate. Science 2003, 302:1044−1046
32. Yasuhara R, Yuasa T, Williams JA, Byers SW, Shah S, Pacifici M, Iwamoto M, Enomoto-Iwamoto M: Wnt/beta-catenin and retinoic acid receptor signaling pathways interact to regulate chondrocyte function and matrix turnover. J Biol Chem 2010, 285:317−327
33. Adams CS, Shapiro IM: The fate of the terminally differentiated chondrocyte: evidence for microenvironmental regulation of chondrocyte apoptosis. Crit Rev Oral Biol Med 2002, 13:465−473
34. Shapiro IM, Adams CS, Srinivas V, Freeman TA: Chondrocyte hypertrophy and apoptosis at the cartialge-bone interface. Edited by Bronner F, Farach-Carson MC. Bone and Osteoarthritis. London, Springer, 2007, pp 109−129
35. MacDonald BT, Tamai K, He X: Wnt/beta-catenin signaling: components, mechanisms, and diseases. Dev Cell 2009, 17:9−26
36. Barker N, Clevers H: Mining the Wnt pathway for cancer therapeutics. Nat Rev Drug Discov 2006, 5:997−1014
37. Wong MH, Rubinfeld B, Gordon JI: Effects of forced expression of an NH2-terminal truncated beta-Catenin on mouse intestinal epithelial homeostasis. J Cell Biol 1998, 141:765−777
38. Ming M, Wang S, Wu W, Senyuk V, Le Beau MM, Nucifora G, Qian Z: Activation of Wnt/beta-catenin protein signaling induces mitochondria-mediated apoptosis in hematopoietic progenitor cells. J Biol Chem 2012, 287:22683−22690
39. Kim K, Pang KM, Evans M, Hay ED: Overexpression of beta-catenin induces apoptosis independent of its transactivation function with LEF-1 or the involvement of major G1 cell cycle regulators. Mol Biol Cell 2000, 11:3509−3523
40. Binari RC, Staveley BE, Johnson WA, Godavarti R, Sasisekharan R, Manoukian AS: Genetic evidence that heparin-like glycosaminoglycans are involved in wingless signaling. Development 1997, 124: 2623−2632
41. Hacker U, Lin X, Perrimon N: The Drosophila sugarless gene modulates Wingless signaling and encodes an enzyme involved in polysaccharide biosynthesis. Development 1997, 124:3565−3573
42. Lin X, Perrimon N: Dally cooperates with Drosophila Frizzled 2 to transduce Wingless signaling. Nature 1999, 400:281−284
43. Dhoot GK, Gustafsson MK, Ai X, Sun W, Standiford DM, Emerson CP Jr: Regulation of Wnt signaling and embryo patterning by an extracellular sulfatase. Science 2001, 293:1663−1666
44. Tao Q, Yokota C, Puck H, Kofron M, Birsoy B, Yan D, Asashima M, Wylie CC, Lin X, Heasman J: Maternal wnt11 activates the canonical wnt signaling pathway required for axis formation in Xenopus embryos. Cell 2005, 120:857−871
45. Fuerer C, Habib SJ, Nusse R: A study on the interactions between heparan sulfate proteoglycans and Wnt proteins. Dev Dyn 2010, 239:184−190
46. Ai X, Do AT, Lozynska O, Kusche-Gullberg M, Lindahl U, Emerson CP Jr: QSulf1 remodels the 6-O sulfation states of cell surface heparan sulfate proteoglycans to promote Wnt signaling. J Cell Biol 2003, 162:341−351
47. Kirkpatrick CA, Dimitroff BD, Rawson JM, Selleck SB: Spatial regulation of Wingless morphogen distribution and signaling by Dally-like protein. Dev Cell 2004, 7:513−523